IOSR Journal of Applied Geology and Geophysics (IOSR-JAGG)
e-ISSN: 2321–0990, p-ISSN: 2321–0982.Volume 6, Issue 5 Ver. II (Sep. – Oct. 2018), PP 59-73
www.iosrjournals.org

Optimizing a Ground Motion Prediction Equation for Low to Moderate Magnitude Velocity Records in Egypt

Yassein. M. H[1],Elkhadrgy. A. A[2],Abuoelela A. Mohamed[1], Hussein. H. M[1] And Mahmoud Sami Soliman [1]

[1]*National Research Institute of Astronomy and Geophysics, Egypt*
2 Geology Department,Faculty of Science /Zagazig University, Egypt
Corresnding author: Yassein.M.H

Abstract: *Ground-motion prediction equations (GMPEs) have been developed for application to shallow crustal earthquakes in tectonically active regions. The objective of this article is to test predictive attenuation relationships for horizontal and vertical peak velocities for small magnitude earthquakes which were recorded in Egypt by Egyptian National Seismological Network (ENSN).More than 2500 velocity records are used in this study with distances up to 150 km from 115 earthquakes recorded by (ENSN) to develop attenuation models, with Mw magnitudes ranging from 3.5 to 5.5.In this study, MATLAB code was developed to modify parameters of attenuation model by using Ambraseys and Halldorsson attenuation models. We found that for PGV, the attenuation relationships decay faster with distance for the vertical component than for the horizontal component.*

Keywords: *GMPEs, Seismic Hazard, ENSN and Ground motion*

Date of Submission: 06-10-2018 Date of acceptance:206-10-2018

I. Introduction

Egypt is located in the northeastern part of the African continent. The general public of population settlements in Egypt are concentrated along a narrow zone of Nile Valley and the Nile Delta. The main factor in terms of seismic hazard is usually associated with the occurrence of moderate size earthquakes near areas highly populated zone. Egypt is characterized by relatively low to moderate seismicity, figure(1) shows the significant earthquakes occurred in Egypt; it has experienced some damage triggered by local shocks throughout its history (i.e. the Cairo 1992 earthquake with Mw = 5.8 in ISC catalog) with an epicenter near Dahshur, 35 km south-west Cairo area. Despite earthquake had a magnitude of 5.8, but was unusually destructive compared to its size, causing 545 deaths, injuring 6,512 and making 50,000 people homeless. Also, large earthquakes that occur at large distances along the northern Red Sea and the two Gulfs of Suez and Aqaba (i.e. Shedwan 1969 earthquake with Mb = 6.1; USGS where the epicenter was located near Shadwan island, southwest of the city of Sharm El Sheikh. At Hurghada, some cracking occurred in the brick walls of a reinforced concrete power plant, and some plaster cracked at some hotels, at Sharm El Sheikh cracks in walls were observed. Areas away from the epicentral area were light to non-existent in damage, though it was felt strongly in the port cities of Safaga and Queseir, and to the west in Qena. In Cairo, one home was destroyed and about ten other homes were damaged with five injuries occurring. The shock was only felt by a few people further to the north in Alexandria. Total damage and casualties amounted to two deaths, fifteen injuries, and seven mosqueswere destroyed (along with around 100 homes Ambraseys, Melville & Adams 2005), the 1995 Gulf of Aqaba earthquake with Mw = 7.2 in ISC where the epicenter was located 60 kilometers south of the head of the Gulf of Aqaba where the countries of Egypt, Israel, Jordan, and Saudi Arabia converge. Damage to buildings occurred in the coastal city of Aqaba, Jordan and a small tsunami was observed by witnesses there. In Nuweiba city , several well-built, modern, concrete reinforced homes were completely destroyed, Klinger et al. 1999,), as well as the Mediterranean offshore the 1955 Alexandria earthquake with Mb = 6.1 by USGS, damage of this earthquake was reported in the Nile Delta between Alexandria and Cairo. About 300 adobe houses were badly damaged around Lake Idku. The earthquake caused 18 deaths and 89 injuries, with 40 houses completely collapsed and about 420 houses ruined, Ambraseys et al, (2005). The seismicity of Egypt was the subject for many authors (e.g., Sieberg 1932, Ismail 1960; Gergawi and El-Khashab 1968; Maamoun et al. 1984; Kebeasy 1990; Ambraseys et al.1994; AbouElenean 1997, 2007; Badawy 1999, 2005; Hussein et. al. 2008). The compilation of an earthquake catalog for the instrumental data, as reported during the time interval 1900–1984, was first achieved by Maamoun et al. (1984). Later on, several efforts where done to enhance and update this catalog (e.g. Elsayedet. Al., 2001, Hussein et. al. 2008).

Ground-motion prediction equations (GMPEs) are fundamental in strong-motion seismology and related tools such as probabilistic seismic hazard analyses, early warning systems, Shake-Maps, the design of structures and earthquake rapid response systems where a Probabilistic Seismic Hazard Analysis (PSHA) is usually carried out to establish a national seismic building code. Peak ground velocity (PGV) is very important to some large structures and buried pipelines.

Ground motion parameters expressed from predictive functional forms relationships reflect the mechanical properties of the ground motions in an abstracted manner. The predictive equation shows the regression of recorded ground motion data to estimate ground acceleration and ground velocity as a function of magnitude, distance and geologic conditions of a site.

However, some general rules should be considered when selecting a proper attenuation model:

(1) The standard deviation of the regression result should be as small as possible.

(2) The attenuation model itself has physical and practical backgrounds.

Large dataset containing a wide range of magnitudes and source-to-site distances are necessarily required to develop GMPE. In low-seismicity regions such as Egypt, the bulk of the data consists of low-magnitude recordings (Mw<5.5). Several studies showed that, due to magnitude scaling problems, equations based on low-magnitude datasets are not able to correctly predict the ground motions of moderate-to-large magnitudes (Mw ≥5; Youngs et al., 1995; Bommer et al., 2007; Cotton et al., 2008).

Some authors believe that ground motions don't vary much regionally, at least for moderate-to-large magnitudes, as long as the same tectonic environment is considered (Bommer, 2006; Stafford et al., 2007). On the opposite side, other authors have highlighted significant regional dependence (e.g., Luzi et al., 2006, for moderate magnitudes in Italy); however, it is often based on restricted regional datasets.

Ground motion prediction equation (GMPE) represents one of the basic pillars in the seismic hazard assessment, some specific localities (e.g., Aswan and Sinai) have been done(Kebeasy et al. (1981), Albert (1986, 1987), Sobaih et al.(1992), El-Sayed et al. (1994), Fat-Helbary and Ohta (1996), and Badawy (1998). Several seismic hazard studies were carried out for Egypt as a whole in addition to several studies for specific localities, Riad et al. (2000), El-Sayed et al. (2001), Fat-Helbary (2003), El-Hefnawy et al. (2006), Deif et al. (2009, 2011), Hamouda (2011a, b), and Mohamed et al.(2012). Table 1 shows preview studies of Seismic Hazard Assessment.

The focused of this study is to evolve GMPEs of Egypt using velocity data of low to moderate magnitudes ranging from 3.5 to 5.5 Mw which is essential for the evaluation of seismic hazard. In this study according to our data magnitude and distances, two GMPE models were tested to find the model which shows the best fitting to the data (Ambraseys et al. 1991 and Halldorsson et al. 2003 models) where these relations used for small magnitude and distances.

II. Dataset And Data Preparation

The dataset used in this study is extracted from the waveform data recorded by Egyptian National Seismological Networks (ENSN). The digital broadband seismographs can directly record ground velocity and therefor can avoid errors of integration to acceleration records. The collected data is about 115 events covering the period from 1998 to 2015 figure (2). All magnitudes are converted to moment magnitudes using the relation of M_w El-Hadidy 2008 because it is directly related to the size of the earthquake source. The magnitude range M_w of these events is from 3.0 to 5.5. Figure (3) shows the magnitude - epicentral distance of the datasets within distances 150 km. After collecting the waveforms recorded by Egyptian National Seismological Network (ENSN), we relocated these events by adding more ENSN stations to increase the accuracy. We approved the hypocenter locations obtained using hypoinverse location code with the least errors in the epicentral horizontal distance (ERH), depth (ERZ) and residuals (RMS) ranging between 0.1 to 0.31 s. This analysis involves the identification and picking off the phase arrival times and the use of S arrival times which greatly improves location accuracy, particularly the hypocentral depth. We relocate earthquake epicenters, estimating their depths and calculating their magnitudes. Events with good azimuth coverage of stations and high signal to noise ratio were selected for this study.

III. Data Processing

All the records have been processed applying a de-trending and band-pass filtering, in the range 0.1–50 Hz. Peak Ground Velocity (PGV) values are measured from velocity records having a signal-to- noise ratio (SNR) greater than 10. The SNR was computed according to the procedure proposed by Vassallo and Cantore (2010), which is based on comparing the pre-event noise amplitude with respect to a portion of the signal centered at the time of occurrence of maximum amplitude.

Our refined dataset comprises about 2500 waveforms (vertical and horizontal components) from 115 events with distances ranging from 0 to 150 km. According to the quality of waveforms and signal to noise ratio, we read the maximum amplitude values as follows:-

(a)The maximum value of the two horizontal PGV components

The maximum value of the two horizontal peak ground velocity components is a_{ns}, a_{ew} selected by:-

$$y_{max} = \max(a_{ns}, a_{ew}) \quad (2)$$

(b)The geometric mean of the two horizontal PGV components

The geometrical mean of the two horizontal ground velocity components a_{ns}, a_{ew} is calculated using the following equation:-

$$y_{ge} = \sqrt{a_{ns} * a_{ew}} \quad (3)$$

(c)The maximum value of the vertical PGV component

The peak vertical ground velocities are measured by reading the maximum value of amplitudes of each vertical component.

In this study we adopted two attenuation model of Ambraseys and Bommer, 1991(equations 5, 6) and Halldórssonand Sveinsson, 2003(equation 7) to our data using the iteration technique.

$$\log(a_h) = -a + bM - \log(r) - c + 0.28P \quad (5)$$

For horizontal component where a =1.09, b= 0.23 and c= 0.0005

$$\log(a_V) = -a + bM - \log(r) - c + 0.27P \quad (6)$$

For vertical component where a =1.34, b= 0.23 and c= 2.7

Where $r^2 = (d^2 + 6.0^2)$, d being the source distance in km and M is the surface-wave magnitude.

$$\log 10(Y) = -a * \log 10(R) + bM - c \quad (7)$$

Where Y is ground motion parameter, a = 1.498, b=0.484, c=0.164, M is moment magnitude and R the distance in km.

The least squares method is a form of mathematical regression analysis that used to find the line of best fit for a dataset and calculate new fitting parameters and create a new attenuation model, providing a visual demonstration of the relationship between the data points. Each point of data is representative of the relationship between a known independent variable and an unknown dependent variable. The least-squares method minimizes the summed square of residuals.

Standard deviation is simply the square root of the variance.

$$SD = \sqrt{\frac{\sum |x - \bar{x}|^2}{n}} \quad (8)$$

Where Σ means the sum of, x is a value in the data set, $\bar{x}$is the mean of the data set and n is the number of data points.

We find that PGV attenuation is faster for the vertical component than the horizontal component. This may be related to the frequency content of the vertical component which is higher than the other components. The results in table (1) show the parameters of the fitted models and their standard deviations and Figures (6, 7 and 8) show the predicted attenuation relations of vertical and horizontal components for Ambeyrases and Halldorsson at various magnitudes

IV. Model Validation

After regressions of the data and estimated new parameters and the standard deviation of each function, we test our model validation in this work using five events with magnitude from 3.6 to 4.6Mw (Table3).

The measured horizontal geometric PGV values, the horizontal maximum PGV values and vertical PGV values from the five events agree with the predicted values estimated from the GMPE relations obtained in this study and have the consistent decay trend.

The estimated of GMPEs in this study (Ambraseys1991 and Halldorsson2003) are dependent on epicentral distance and magnitude. These relations are investigated and both the median value and the median ±σ, the standard deviation, are shown for each model which reflects the range reading might exit (figures 4 and 5).

From figures (9, 10, 11, and 12), we compared the results of the two models. We noticed that geometrical mean of Ambraseys model fewer data points (3%) are located outside the standard deviation compared to Halldorsson model (4%). On the other hand, distribution of maximum PGV data points of Halldorsson model fewer data points fall outside the standard deviation (3%) compared with Ambraseys model shows (6%). For vertical components of Halldorsson model (10%) which fewer data points are located outside SD compared to Ambraseys model (19%).

We also analyzed the residuals for PGV with respect to calculated GMPEs relation constructed in this study. We define the residuals (RES) as

$$RES = \log Y^{obs} - \log Y^{pred} \quad (9)$$

where Y^{obs} and Y^{pred} represent the observed and predicted peak velocity values, respectively, the predicted values being estimated through the GMPE relation for the two models.

The deviations of the data residuals from the predicted attenuation relationships are shown in Figures (13 and 14). These figures show the ratio of the logarithm of observed data to the logarithm of the predicted value. The ratio is called the total error. In this study the common logarithmic scale is used. The figures show that the error is log-normally distributed. The standard deviations are 0.539 for maximum PGV and 0.477 for geometrical PGV for modified Halldorsson model and 0.5407 for maximum PGV and 0.4756 for geometrical PGV for the modified Ambraseys model. These histograms provide complimentary insights on the fit between the models and data. Most recording data from events were distributed within the range between plus and minus one standard deviation of the mean attenuation curve.

V. Conclusion

In this paper, the velocity records collected from Egyptian National Seismological Network (ENSN). The attenuation models for the horizontal and vertical peak velocity are acquired using Ambraseys and Halldorsson models. According to the study, the model is applicable on the conditions by regression with magnitudes from 3.5 to 5.5 Mw within epicentral distance up to 150 km. Then verification is made with the five earthquakes recorded recently by ENSN. It is apparent from the results that the calculated attenuation relations are basically consistent with the original records. The measured horizontal geometrical PGV values, the horizontal maximum PGV values and vertical PGV values from the five events agree with the predicted values estimated from the GMPE relations obtained in this study. We noticed that geometrical mean of Ambraseys model fewer data points are located outside the standard deviation compared to Halldorsson model. On the other hand, distribution of maximum PGV data points of Halldorsson model fewer data points fall outside the standard deviation compared with Ambraseys model. For vertical components of Halldorsson model which fewer data points are located outside SD compared to Ambraseys model.

References

[1]. **AbouElenean, K. 1997:**Seismotectonics of Egypt in relation to the Mediterranean and Red Sea tectonics. Ph.D. Dissertation, Ain Shams University, Egypt.

[2]. **Akkar, S., and Bommer, J. J. 2007:** Prediction of elastic displacement response spectra in Europe and the Middle East, Earthq. Eng. Struct.Dynam. 36, 1275–1301.

[3]. **Albert, R.N.H. 1986:** Seismicity and earthquake hazard at the proposed site for a nuclear power plant in the El-Dabaa area, north western desert, Egypt. ActaGeophys Pol 34:263–281.

[4]. **Albert, R.N.H. 1987:** Seismicity and earthquake hazard at the proposed site for a nuclear power plant in the Anshas area, Nile delta, Egypt. ActaGeophys Pol 35:343–363

[5]. **Ambraseys,N. N., and Bommer J. J. 1991:**The Attenuation of Ground Accelerations in Europe. Earthquake Engineering and Structural Dynamics, Vol. 20. 1179-1202 (1991)

[6]. **Ambraseys, N. N., Douglas, J., Sarma, S. K., andSmit, P. M. 2005:**Equations for the estimation of strong ground motions from shallow crustal earthquakes using data from Europe and the Middle East: Horizontal peak ground acceleration and spectral acceleration, Bull. Earthq. Eng. 3, no. 1, 1–53.

[7]. **Ambraseys, N.N., Melville, C.P., Adams, R.D. 1994:** The Seismicity of Egypt, Arabia and the Red Sea: A Historical Review, Cambridge University Press, ISBN 978-0521020251.

[8]. **Badawy, A. 1998**: Earthquake hazard analysis in northern Egypt. ActaGeodaeticaetGeophysicaHungarica 33:341–357

[9]. **Badawy,A.2005**: Present-day seismicity, stress field and crustal deformation of Egypt J. Seismol., 9 (2005), pp. 267-276

[10]. **Badawy.A., and Horvath, F.2005:** Recent stress field of the Sinai subplate region Tectonophysics, 304 (1999), pp. 385-403

[11]. **Bommer, 2006:** Re-thinking seismic hazard mapping and design return periods, in First European Conference on Earthquake Engineering and Seismology, Geneva, Switzerland, 3–8 September 2006, Paper 1304.

[12]. **Cotton, F., Pousse, G., Bonilla, F., and Scherbaum, F. 2008:** On the discrepancy of recent European ground motion observations and predictions from empirical models: Analysis of KiK-net accelerometric data and point-source stochastic simulations, Bull. Seismol.Soc. Am. 98, 2244–2261.

[13]. **Deif, A., AbouElenean, K., El-Hadidy, M., Tealeb, A., andMohamed, A. 2009:** Probabilistic seismic hazard maps for Sinai Peninsula, Egypt. J GeophysEng 6:288–297

[14]. **Deif, A., Hamed, H., Igrahim, H.A., AbouElenean, K., and El-Amin, E.M. 2011:** Seismic hazard assessment in Aswan, Egypt. J GeophysEng 8:531–548

[15]. **El-Hefnawy, M., Deif, A., El-Hemamy, S.T., and Gomaa, N.M. 2006:** Probabilistic assessment of earthquake hazard in Sinai in relation to the seismicity in the eastern Mediterranean region. B EngGeol Environ 65:309–319

[16]. **El-Sayed A, Vaccari V, Panza GF (2001):** Deterministic seismic hazard in Egypt. Geophys J Int 144:555–567

[17]. **El-Sayed, A., Wahlstro¨m, R., andKulha´nek, O. 1994:** Seismic hazard of Egypt. Nat Hazards 10:247–259

[18]. **Fat-Helbary, R.E. 2003:** Probabilistic analysis of potential ground motion levels at the principal cities in Upper Egypt. J ApplGeophys 2:279–286

[19]. **Fat-Helbary, R.E., and Ohta, Y. 1996**: Assessment of Seismic Hazard in Aswan Area, Egypt. In: 11th World conference on earthquake engineering. Paper No. 136 Published by Elsevier Science Ltd

[20]. **Gergawi, A., and El-Khashab, H., 1968:** Seismicity of U.A.R. Helwan Obs. Bull. 76.

[21]. **Halldorsson, P., and Sveinsson, B. I. 2003:**Dvinunhrodunar a Islandi. Tech. rept. 03025.Vedurstofa Islands (Icelandic Meteorological Office).

[22]. **Hamouda, A.Z. 2011a:** Recent evaluation of the assessment seismic hazards for Nuweiba, Gulf of Aqaba. Arab J Geosci 4:775–783

[23]. **Hamouda AZ (2011b):** Assessment of seismic hazards for Hurghada, Red Sea, Egypt. Nat Hazards 59:465–479

[24]. **Hussein, H.M., Hurukawa, N., Al-Arifi, N.S., 2008.** Relocation of microearthquakes in Abu Dabaab region, Egypt using Modified Joint Hypocenter Determination Method.Individual study, International Institute of Seismology and Earthquake Engineering, Tsukuba, Japan.

[25]. **Ismail A., 1960 :** " Near and local Earthquakes of Helwan (1903-1950), Helwan , Bull.,pp 49,32

[26]. **Kebeasy RM, Maamoun M, Albert RNH (1981)** Earthquake activity and earthquake risk around the Alexandria area in Egypt. ActaGeophys Pol 29:37–48.

[27]. **Kebeasy, R.1990:** Seismicity of Egypt. In; Said, R.(Editor), Geology of Egypt, A.A. Bakema,

[28]. **Klinger., Yann., Rivera., Luis.,Haessler., Henri.,Maurin., Jean-Christophe :August 1999:** "Active Faulting in the Gulf of Aqaba: New Knowledge from the Mw 7.3 Earthquake of 22 November 1995"(PDF), Bulletin of the Seismological Society of America, Seismological Society of America, 89 (4): 1025–1036

[29]. **Luzi, L., Morasca, P.,Zolezzi, F.,Bindi, D.,Pacor, F.,Spallarossa, D., and Franceschina, G. 2006:** Ground motion models for Molise region (southern Italy), in Proc. of the First European Conference on Earthquake Engineering and Seismology (a Joint Event of the 13th ECEE and 30th General Assembly of the ESC), Paper No. 938, Geneva, Switzerland, 3–8 September, 2006, 10 pp.

[30]. **Maamoun, M., Allam, A., andMegahed, A. 1984:** Seismicity of Egypt. Bulletin of Helwan Institute of Astronomy and Geophysics, 109–160.

[31]. **Mohamed, A.A., El-Hadidy, M., Deif, A., and AbouElenean, K. 2012:** Seismic hazard studies in Egypt. NRIAG J AstronGeophys 1:119–140

[32]. **[32]National Geophysical Data Center / World Data Service (NGDC/WDS) Significant Earthquake Database,**Boulder,CO,USA.(Availableat http://www.ngdc.noaa.gov/nndc/struts/form?t=101650&s=1&d=1)

[33]. **Riad, S., Ghalib, M., El-Difrawy, M.A., Gamal, M. 2000:** Probabilistic Seismic Hazard Assessment in Egypt. Ann GeolSurv Egypt 23:851–881
Rotterdam, Netherland.

[34]. **Sieberg, A. 1932**:Erdbebengeographie. Handbuch der Geophysik, Band IV, Abschnitt VI, Berlin, Germany.

[35]. **Sobaih, M.E., Kebeasy, R.M., and Ahmed, K.A. 1992:** Development of seismic hazard maps for Egypt. Int J EarthqEng 2:33–58

[36]. **Stafford, P. J., F. O. Strasser, and J. J. Bommer (2007).** An evaluation of the applicability of the NGA models to ground-motion prediction in the Euro-Mediterranean region, Bull. Earthq. Eng. 6, doi: 10.1007/s10518-007-9053-2.

[37]. **Vassallo, M., and Cantore, L. 2010:** Analisi del rumoresismico, in MetodieTecnologie per l'Early-warningSismico, Iannaccone, G.,and Zollo, A.(Editors),Doppiavoce, 85–115, ISBN: 978-88-89972-20-5.

[38]. **Youngs, R. R., Abrahamson, N., Makdisi, F. I., andSadigh, K. 1995**. Magnitude-dependent variance of peak ground acceleration. Bulletin of the Seismological Society of America, **85**(4), 1161–1176.

Figure (1) significant earthquakes in Egypt

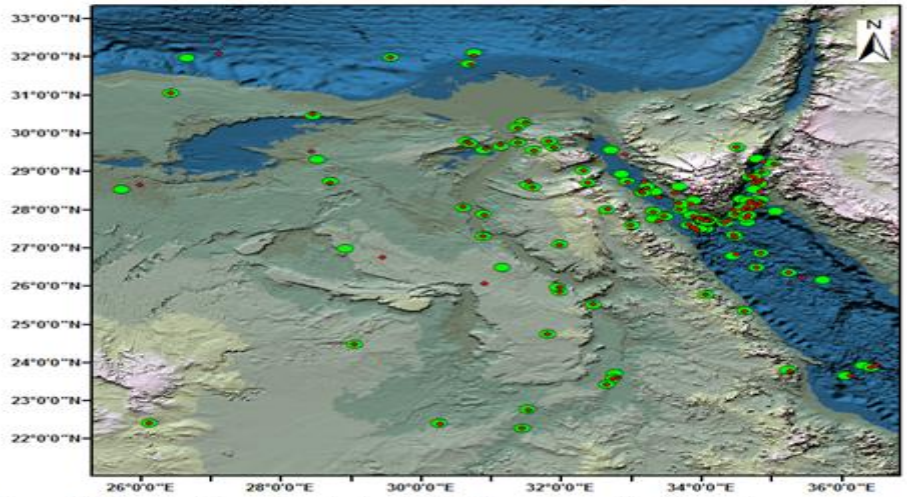

Figure (2): Located (green) and relocated (red) events used in this study

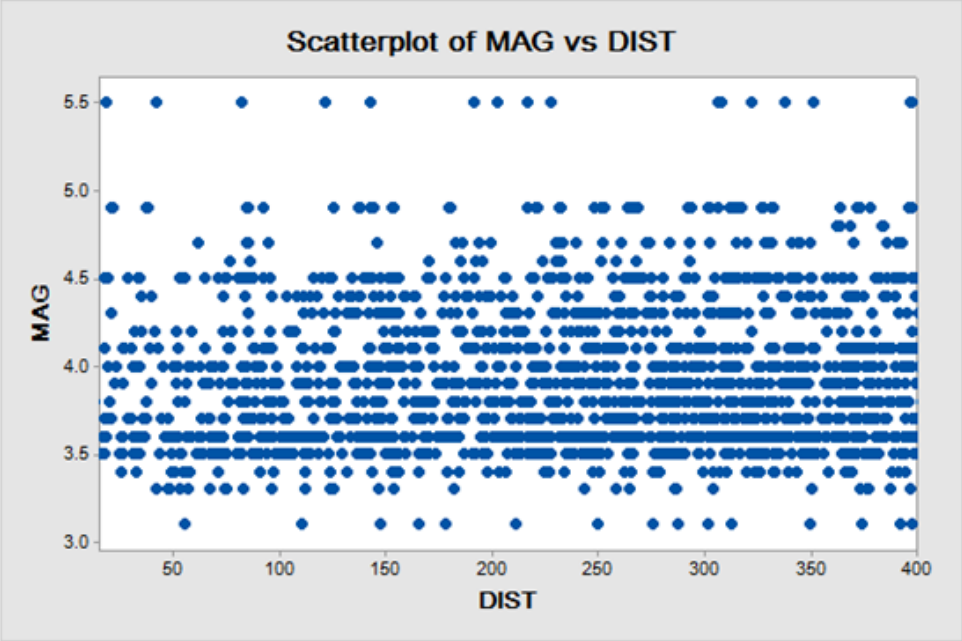

Figure (3) Magnitude - epicentral distance distribution

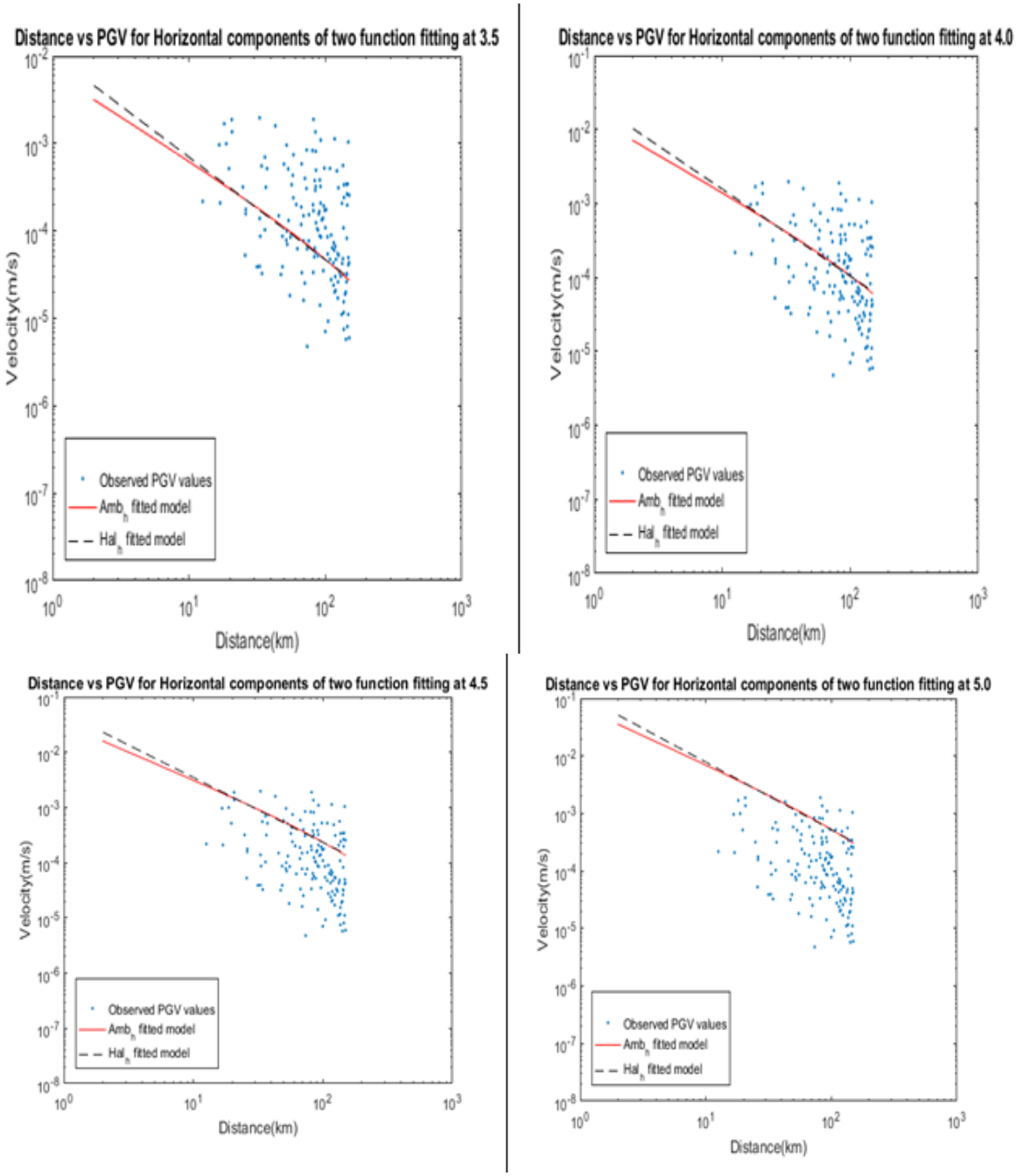

Figure (4) Ambraseys and Halldorsson prediction models for the horizontal PGV at 3.5, 4.0, 4.5 and 5.0 moment magnitude

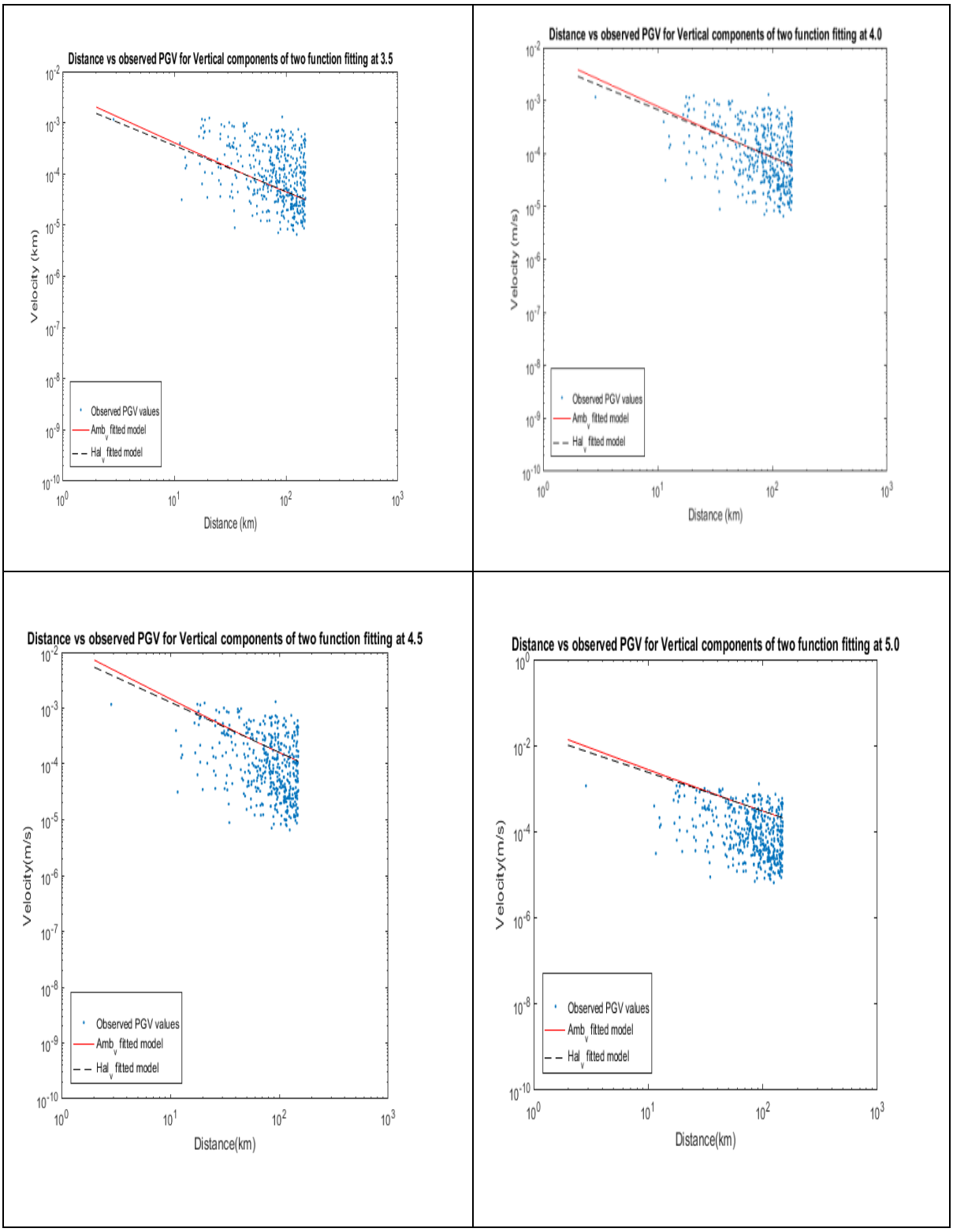

Figure (5) Ambraseys and Halldorsson prediction models for the vertical PGV at 3.5, 4.0, 4.5 and 5.0 moment magnitude

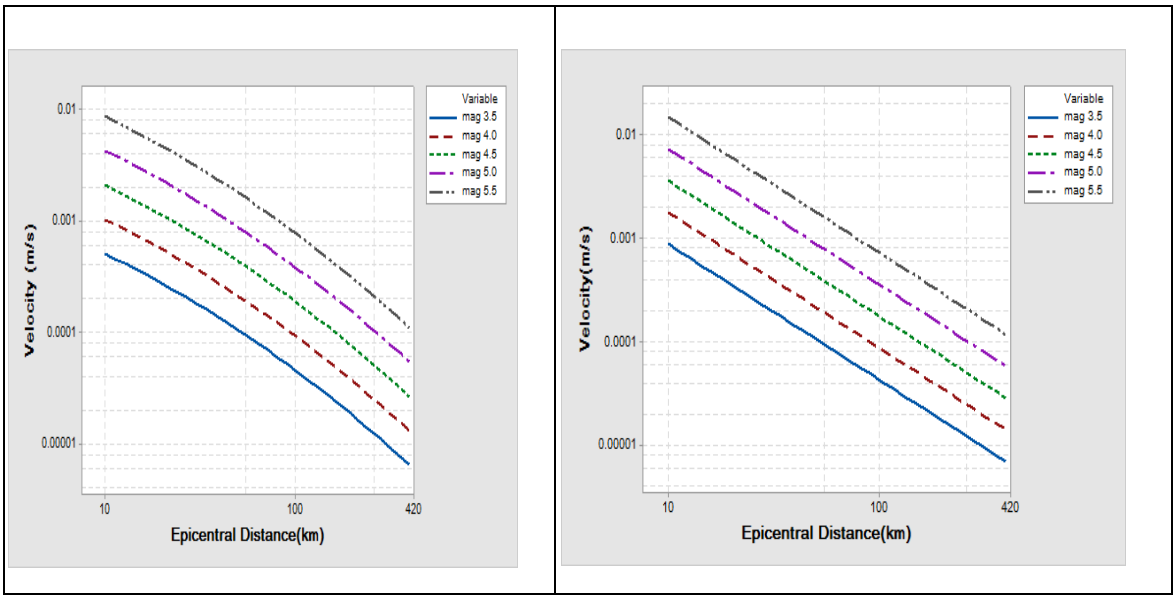

Figure (6) Predicted horizontal maximum PGV attenuation curves for Ambraseys (left) and Halldorsson (right) model with respect to epicentral distance for magnitudes Mw=3.5, 4.0, 4.5, 5.0, 5.5

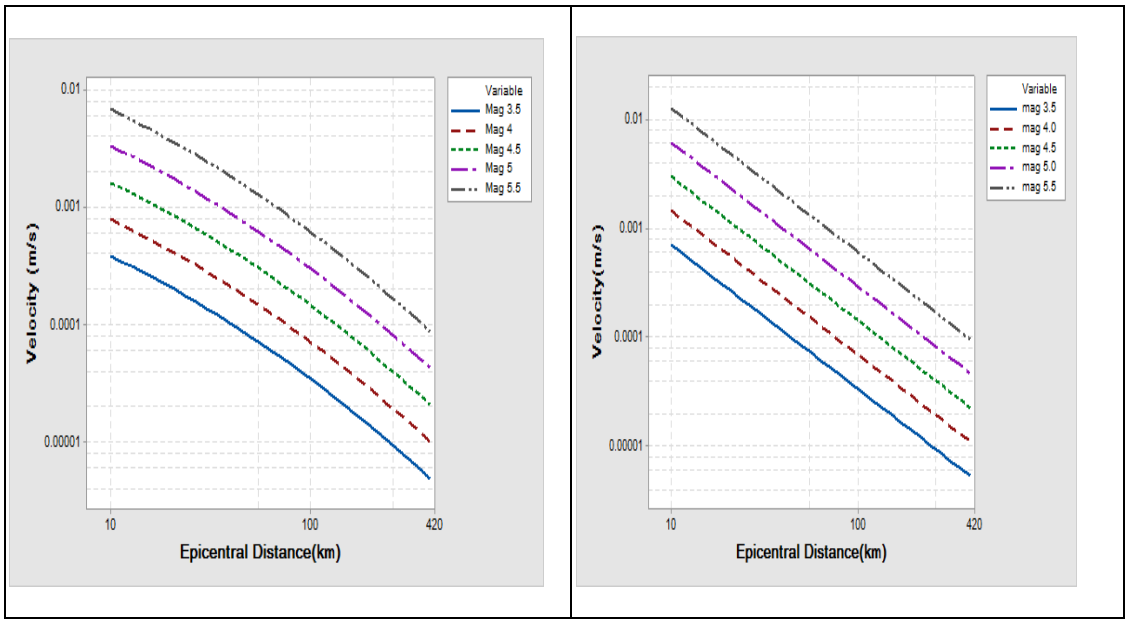

Figure (7) Predicted horizontal geometric PGV attenuation curves for Ambraseys (left) and Halldorsson (right) model with respect to epicentral distance magnitudes Mw=3.5, 4.0, 4.5, 5.0, 5.5

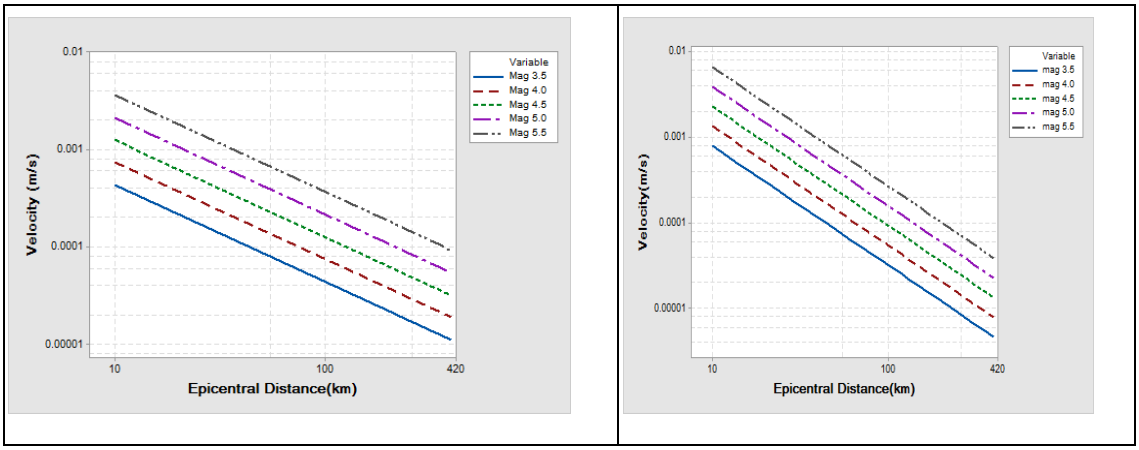

Figure (8) Predicted vertical PGV attenuation curves for Ambraseys (left) and Halldorsson (right) model with respect to epicentral distance magnitudes Mw=3.5, 4.0, 4.5, 5.0, 5.5

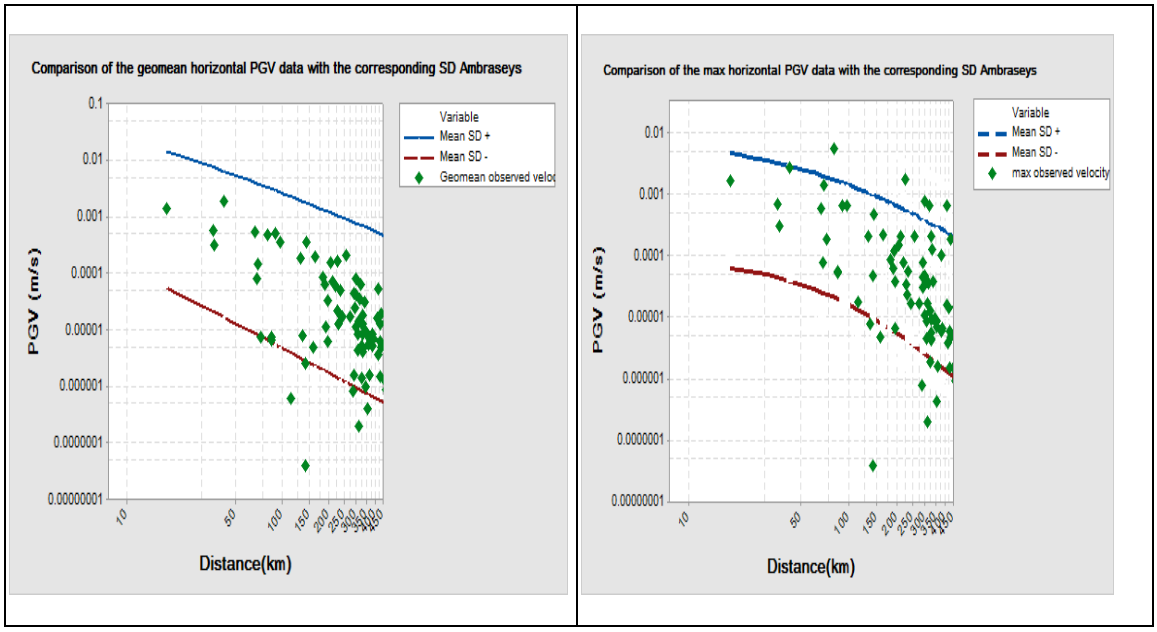

Figure (9) Comparison of geometrical mean (left) and maximum (right) PGV distribution for Ambraseys withStandard Deviation for tested events

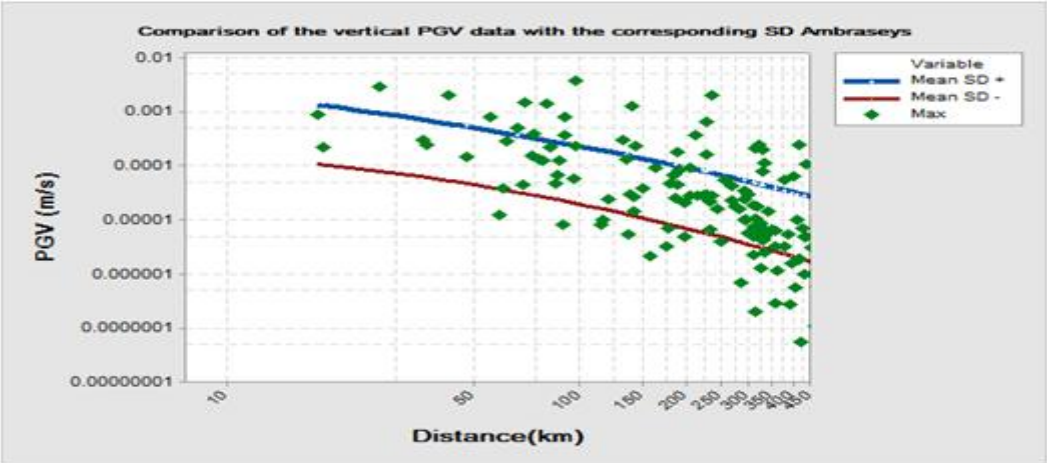

Figure (10) Comparison of PGV (vertical components) distribution for Ambraseys model with standard deviation for tested events

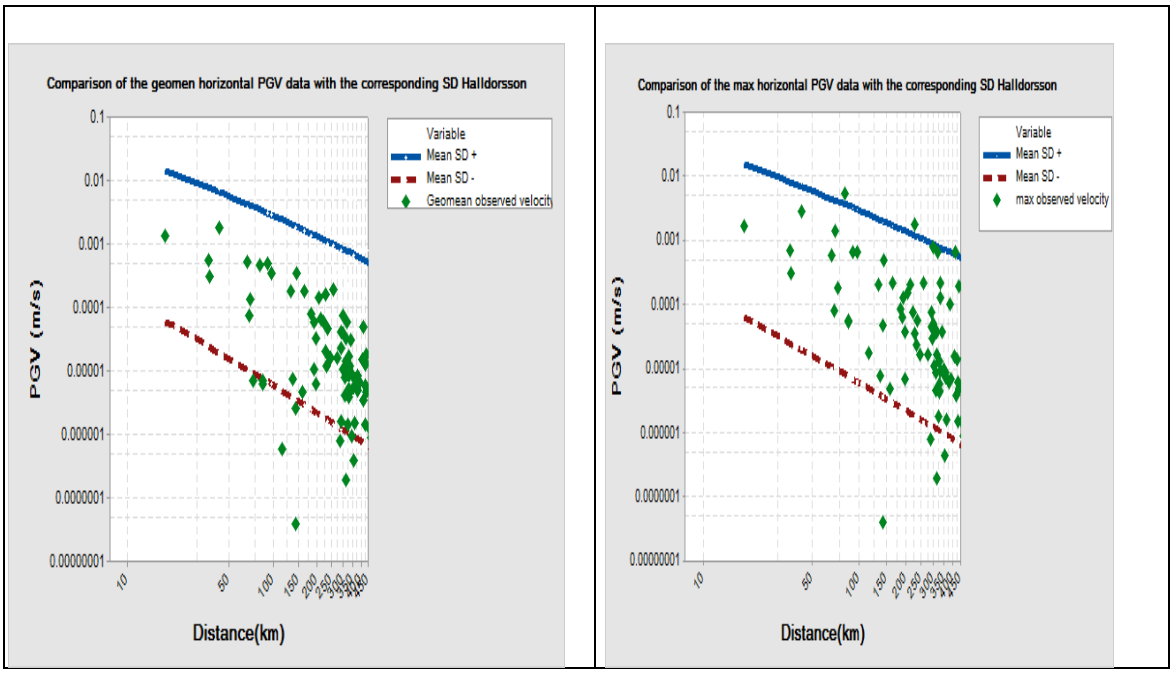

Figure (11) Comparison of the geometrical mean (left) and maximum (right) PGV for Halldorsson model with standard deviation for tested events

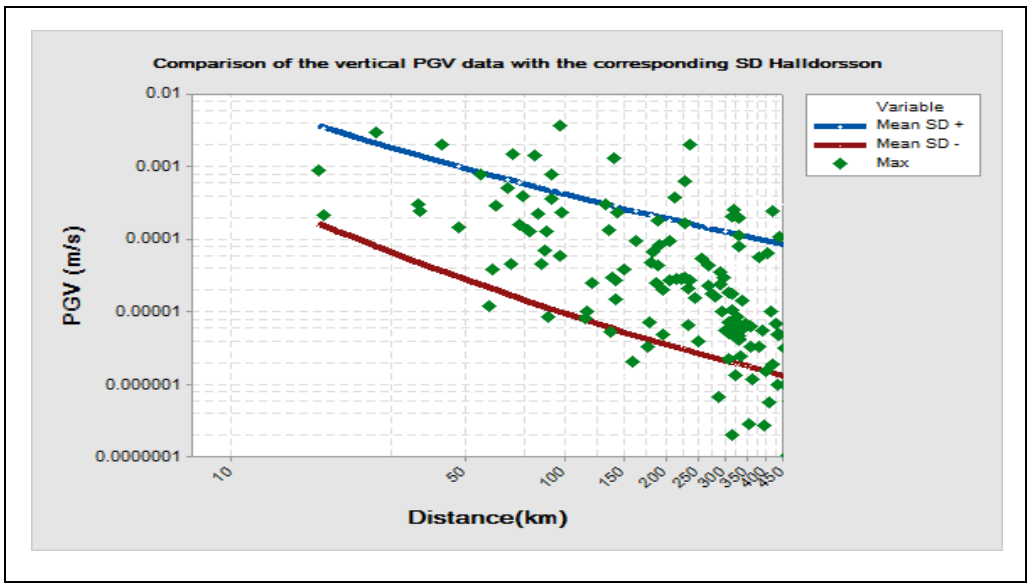

Figure(12) Comparison of PGV (vertical components) distribution for Halldorsson model with standard deviation for tested events

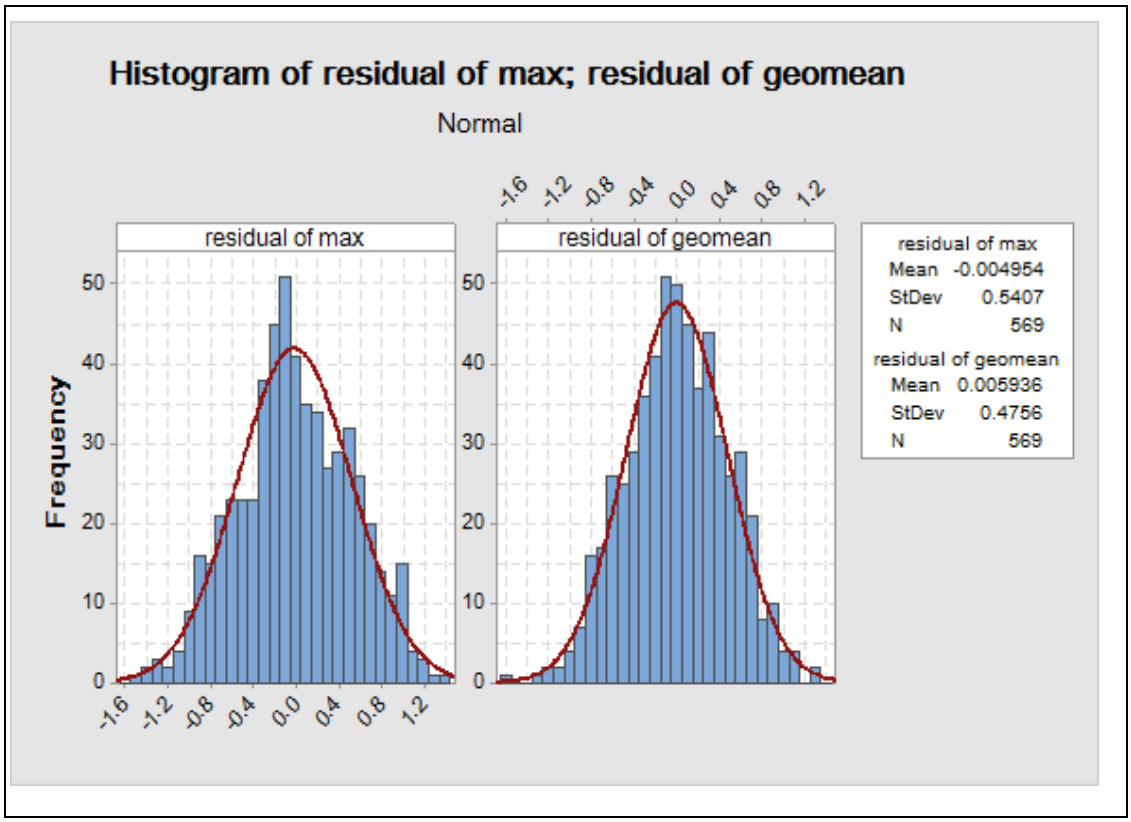

Figure (13) Residual distributions for maximum (left) and geometrical mean (right) PGV values of Ambraseys model

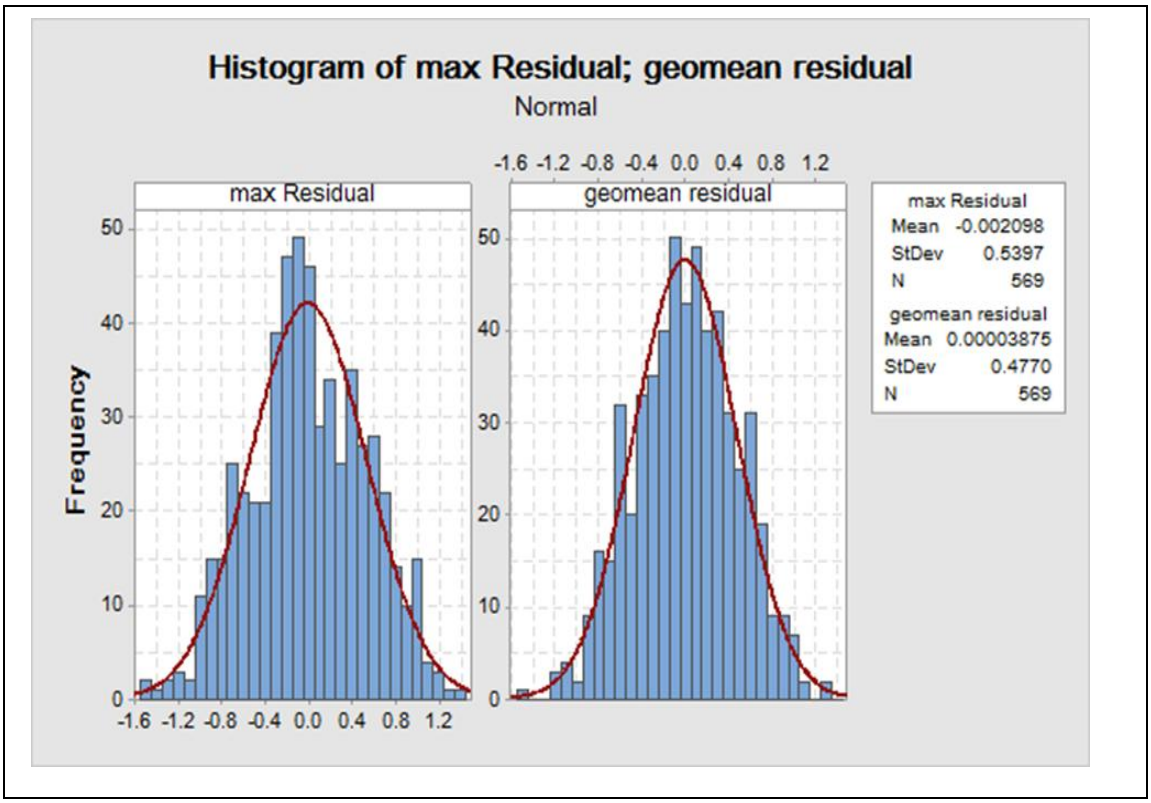

Figure (14) Residual distributions of maximum (left) and geometrical mean (right) values of PGV forHalldorsson model

Table 1 Description of the seismic hazard assessments done upon different regions in Egypt

The study	Study region	Earthquake catalogue	Attenuation relationship	Results
Sobaih et al.(1992)	Whole Egypt	Helwan station catalogue (1908–1984), Maamoun et al. (1984), ISC bulletin (1910–1984), and USGS bulletin (1903–1984)	Maamoun et al. (1984)	PGA values with a Probability of exceedance of 10, 15 and 20 % in 50, 100, and 500 years. Hazard curves for 4 cities were provided
El-Sayed and Wahlstro¨m (1996)	Whole Egypt	Historical events compiled from Ambraseys (1961, 1978, and 1983) and Poirier and Taher (1980). Instrumental events (1900–1993) compiled from ISC bulletin, NEIC, IPRG, Maamoun et al. (1984) and ENSN	Maamoun et al. (1984)	Intensity values to occur in a time period of 94 years with a probability of exceedance of 10 and 80 %
Fat-Helbary and Ohta (1996)	Aswan area	Compiled from Maamoun et al. (1984) and Aswan bulletin	Fat-Helbary (1994)	PGA values with a 10 % probability of exceedance in 100 years
Badawy (1998)	Northern Egypt	Historical events compiled from Kebeasy (1990), Maamoun and El-Khashab (1978), and El-Gamal et al. (1993). Instrumental events (until 1995) compiled from ISC bulletin and ENSN	Maamoun (1979) and Badawy (1998)	Expected intensity maps with a 10, 15 and 20 % probability of exceedance in 1 year
Fat-Helbary (1999)	Whole Egypt	Historical events compiled from Ambraseys et al. (1994). Instrumental events (1900-1998) obtained by Maamoun et al. (1984), ISC bulletin, NEIC/PDE, Helwan and Aswan bulletins	Makropoulos and Burton (1985)	Expected intensity maps for return periods of 50 and 100 years, PGA values with a 10 % probability of exceedance in 50 and 100 years, and hazard curves for 13 cities
Riad et al. (2000)	Whole Egypt	Historical events compiled from Maamoun (1979), Maamoun et al. (1984), Ben-Menahem (1979), and WCC (1985). Instrumental data (1900–1996) obtained by Makropoulos and Burton (1981), Maamoun et al. (1984), Ben-Menahem (1979), WCC (1985), Riad and Meyers (1985),IPRG, and NEIC	Campbell (1981) for shallow earthquakes and Crouse (1991) for intermediate activity	PGA values with a 10 % probability of exceedance in 10, 25, 50, 100 and 250 years
El-Sayed et al. (2001)	Whole Egypt	Historical data compiled from Ambraseys et al. (1994) and Poirier and Taher (1980). Instrumental data (1900–1998) obtained by EMSC, ISC, IPRG, PDE/ NEIC, Maamoun et al. (1984), CMT, and AbouElenean (1993)	Computation of synthetic seismograms at a set of grid points	Peak displacement, peak velocity, and design ground acceleration values
Fat-Helbary and Tealeb (2002)	Kalabsha (Aswan)	Aswan annual bulletin	Fat-Helbary and Ohta (1996)	Hazard curves for 6 sites
Fat-Helbary (2003)	Upper Egypt	ENSN and Aswan annual bulletins (1900–2001)	Makropoulos and Burton (1985)	Hazard curves for 8 cities in Upper Egypt
El-Hefnawy et al. (2006)	Sinai Peninsula	Historical events taken from Ambraseys et al. (1994). Instrumental data (till 2003) compiled from ISC bulletin, Papazachos and Papazachos (1997), ENSN, and IPRG	Joyner and Boore (1981)	PGA values with a 10 % probability of exceedance in 50 and 100 years
El-Adham and El-Hemamy (2006)	El-Dabaa (Northern Western Desert)	Data compiled from NEIC, EMSC (1902–1985), ISC (1964–1996), Maamoun et al. (1984) and ENSN	Joyner and Boore (1981)	PGA values with a 10 % probability of exceedance in 50, 100, 450 years
Fat-Helbary et al.(2008)	Tushka (West of Aswan)	Data taken from Maamoun et al. (1984), ISC, NEIC, PDE and Aswan bulletin (1982–2008)	Makropoulos and Burton (1985)	PGA values for 475 years return period, and a hazard curve for New-Tushka city
Deif et al.	Sinai Peninsula	Historical data taken from Ambraseys	Ambraseys et al.	PGA and SA (for

(2009)		et al. (1994). Instrumental data (1900–2006) compiled from IPRG, AbouElenean (1997), ENSN, Ambraseys and Adams (1993) and ISC	(1996)	0.2,0.5, 1.0 and 2.0 s) values for 475 years return period, and UHS for 4 cities
Deif et al. (2011)	Aswan area	Data (1900–2009) compiled from Ambraseys et al. (1994), EHB, ISC (2011), NEIC, CMT, AbouElenean (1997), ENSN (1998– 2010) and Aswan bulletin	Ambraseys et al. (1996), Abrahamson and Silva (1997) and Boore et al. (1997) in a logic tree approach	PGA and SA (for 0.1, 0.2, 0.3, 0.5, 0.8, 1.0 and 2.0 s) values for 475 years return period, UHS for return periods of 475 and 2475 years, deaggregation plots (for 0.1, 0.2, 1.0 and 2.0 s) for return periods of 475 and 2475 years
Hamouda (2011a)	Nuweiba (Gulf of Aqaba)	Historical data compiled from Ambraseys et al.(1994) and Ambraseys (2001). Instrumental data (1900–2006) compiled from ISC (2011), NEIC, NOAA and ENSN(1998–2010) bulletin	Atkinson and Boore (1995,1997)	Expected magnitudes curves and PGA values for different probability levels of exceedance
Hamouda (2011b)	Hurghada (Red Sea)	Historical data compiled from Maamoun et al. (1984), Ambraseys et al. (1994), Ambraseys (2001) and Badawy (2005). Instrumental data (1900–2005) compiled from ISC (2011), NEIC, NOAA and ENSN(1998–2010) bulletins	Atkinson and Boore (1995)	Expected magnitudes curves and PGA values for different probability levels of exceedance
Mohamed et al. (2012)	Whole Egypt	Historical data compiled from Ambraseys et al. (1994), Poirier and Taher (1980), Maamoun et al. (1984), Badawy (1998) and Badawy et al. (2010). Instrumental data (1900–2009) compiled from PDE, NEIC, ISC (2011), EHB, CMT, Papazachos and Papazachou (2003), AbouElenean (1997) and ENSN (1998–2010)	Abrahamson and Silva (1997), Boore et al. (1997), Campbell and Bozorgnia (2003), and Campbell and Bozorgnia (2008) for shallow sources, and Youngs et al. (1997) and Zhao et al. (2006) for intermediate sources.	PGA and SA (for 0.1, 0.2, 0.3, and 1.0 s) values for 475 and 2475 years return periods, and UHS (72, 475, 975 and 2475 return periods) for 7 cities.

Table (2) Modified parameters for Ambraseys attenuation model with Standard Deviation (SD) of each parameter

	a	b	c	
New parameters	-4.4177	0.6173	-0.0009	Maximum horizontal components
SD	0.4213	0.1077	0.0004	
New parameters	-4.5722	0.6273	-0.0009	Geometrical mean horizontal components
SD	0.4347	0.111	0.0004	
New parameters	-4.1205	0.4956	-0.0011	Vertical components
SD	0.2443	0.062	0.0002	

Table (3) Modified parameters for Halldorsson attenuation model with Standard Deviation (SD) of each parameter

	a	b	c	
New parameters	0.6154	-1.3134	-3.9001	Maximum horizontal components
SD	0.1088	0.1708	0.5313	
New parameters	0.6291	-1.3274	-4.0276	Geometrical mean horizontal components
SD	0.1118	0.1737	0.5441	
New parameters	0.4943	-1.3909	-3.472	Vertical components
SD	0.0627	0.1003	0.3156	

Table (4) source parameters of events used for testing modified models

No	Year	month	day	h	m	sec	Latitude	longitude	Depth	Mw
1	2014	07	18	20	01	30.46	30.05	32.24	20	4.3
2	2016	12	27	01	48	02.44	28.56	34.67	17	4.2
3	2017	01	21	16	54	25.43	30.24	31.93	4	3.8
4	2017	02	09	22	30	33.34	28.18	34.58	4	3.6
5	2017	05	19	14	16	21.7	27.94	34.56	3	4.6

Yassein.M.H "Optimizing a Ground Motion Prediction Equation for Low to Moderate Magnitude Velocity Records in Egypt "IOSR Journal of Applied Geology and Geophysics (IOSR-JAGG) 6.5 (2018): 59-73.